

# Theory of Characteristics Mode Based Design of a Planar Monopole Antenna with Polarization Diversity for FSS and SAR Application



Reshmi Dhara

**Abstract** Here, using Theory of characteristics Mode (TCM) a single feed planar monopole antenna is demonstrated. After TCM analysis dominant modes of the radiator are identified. Using appropriate feeding method and modified ground plane the dominant modes are excited to achieve quad impedance band (IB) with polarization diversity characteristics. The design antenna which is proposed here involves two L-shaped radiators with two asymmetric cross slots within it creates mutual coupling to attain dual circularly polarized (CP) bands. To generate quad impedance bandwidth (IBW) defective ground plane is utilized on the reverse side of the substrate. The proposed antenna covered the quad simulated IBs are from 3.631–4.167, 6.542–8.494 GHz, 8.859–10.253 GHz and 10.8494- beyond 15 GHz respectively. The simulated dual ARBW's span over 3.865–4.069 GHz within 1<sup>st</sup> IB and 8.888–9.785 GHz within 3<sup>rd</sup> IB. This antenna can be used for S- and X-band, particularly Fixed Satellite Service (FSS) and Synthetic Aperture Radar (SAR) applications.

**Keywords** TCM · Quad band · Polarization diversity · Axial ratio bandwidth · Impedance bandwidth · FSS · SAR

## 1 Introduction

Recently, multi band antennas with polarization diversity have satisfied multiple necessities of many devices in wireless communication systems. In personal mobile and global position system (GPS) devices, antennas through omni-directional radiation are particularly suitable. On the other hand, several communication devices for example global navigation satellite systems, point-to-point communication systems, and other satellite communication systems, antennas with unidirectional radiation patterns are growing by means of an integral technology. To generate vertically/horizontally omni-directional dual-polarized radiation it's needed to superimposed two radiations from a vertically polarized monopole antenna and a horizontal

---

R. Dhara (✉)

Department of Electronics and Communication Engineering, National Institute of Technology Sikkim, South Sikkim, Ravangla 737 139, India  
e-mail: [reshmidhara@nitsikkim.ac.in](mailto:reshmidhara@nitsikkim.ac.in)

polarized loop antenna. Now in communication system where the astronomical research is the main attention, several uses communication devices are essential as a substitute to single communication typical device. As a consequence of the striking characteristics like lower footprint, simpler geometry, and lighter in weight, planar monopole antennas help as an utmost suitable practise. This is known to all that a conventional monopole antenna in longitudinal direction creates linearly polarized (LP) wave. But the foremost drawbacks of LP wave expected at dual-band process are lower sensitivity, multipath fading to the positioning between the transmitting and receiving antennas, lower mobility, and like that [1–3]. This could be overwhelmed to a great scope consuming the circularly polarized antennas. Henceforth, dual band antennas by means of two different frequency bands instantaneously functioning dual circular polarization (left hand circular polarization (LHCP) and right-hand circular polarization (RHCP)), are significantly widespread over dual band antennas with two orthogonal (vertically/horizontally) linear polarizations. The requirement of multiple antennas decreases due to using a multiband antenna with dual polarization characteristics. The CP antenna is very attractive for many wireless systems as no strict orientation between transmitting and receiving antenna is required and encountering interference. To fulfilments these necessities of multi band antenna presentation together linear and circular polarization, various methodologies have been used by many researchers [4–8].

TCM analysis is a great tool which give the analyzation of existing dominant modes within the radiator at the desired resonant frequency. However, the TCM analysis is lacking in previously reported literature for the multiband antennas. Here, the proposed CP antenna also utilizes the analysis of TCM tools for the multi impedance bands and polarization diversity characteristics.

Inspired by the aforementioned the whole thing, a simple quad band monopole antenna with LHCP in 1<sup>st</sup> band, LP in 2<sup>nd</sup>, LHCP in 3<sup>rd</sup> and LP in 4<sup>th</sup> bands are proposed in this paper. The proposed design can support 3.631–4.167 GHz (535.6 MHz,  $f_{rc1} = 3.9$  GHz, 13.73%), 6.542–8.494 GHz (1951.8 MHz,  $f_{rc2} = 7.52$  GHz, 25.96%), 8.859–10.253 GHz (1134.3 MHz,  $f_{rc3} = 9.56$  GHz, 14.59%) and 10.8494- beyond 15 GHz (4150.6 MHz,  $f_{rc4} = 12.92$  GHz, 32.19%). The simulated dual ARBW's span over 3.865–4.069 GHz (203.7 MHz,  $f_{cp1} = 3.97$  GHz, 5.14%) within 1<sup>st</sup> IB and 8.888–9.785 GHz (897.3 MHz,  $f_{cp2} = 9.34$  GHz, 9.6%) within 3<sup>rd</sup> IB. To design a quad antenna, it has been appropriately improved in a method so that it can sustenance together linear and circular polarizations.

An actual good reflection coefficient, widespread ARBW and dependable radiation features are gained for the implemented antenna. It became apparent that the implemented antenna is simple and make available for wider LP, CP frequency bands.

This paper is presented like: Sect. 2: Design Procedure of Antenna; Sect. 3: Simulation Justifications and Discussions; and lastly Sect. 4: Conclusion.

## 2 Design Procedure of Antenna

### Design of the Radiator

The progress steps of the radiator are represented in Fig. 1. The reflection coefficient and axial ratio bandwidth progress plots of the designed radiator are shown in Figs. 2(a) and (b). First in Antenna.1 is designed at a resonating frequency 3.6 GHz using a rectangular radiator and a ground plane rectangular in size on the reverse side of the substrate for FSS application. Here a centre feed microstrip line is utilized to fed the antenna. But the IBW is very poor at this frequency and also got a CP in the higher frequency region (12.8 GHz). To improve the IBW and to satisfy the multiband characteristics by using the same dimension of the antenna its need to create additional current paths. For that reason, two L-shaped radiators are used by modifying the rectangular shaped radiator. The gap between two radiators create a coupling effect [9], due to generation of capacitance between them. This gap creates additional current path that increase IBW in addition to improve ARBW performance compared to earlier stage. To improve ARBW performance more also an asymmetric feed [8] is used in this step. Better impedance matching network can be performed by using this feeding structure. But this Antenna.2 generate only a small CP (9.89 GHz) band. In next stage for improving the ARBW performance more, two slots asymmetric in size [10–12] are edged from two L-shaped radiator gives Antenna.3. These two slots generate two very small CP bands resonating at frequency 3.78 GHz and 9.4 GHz respectively. These asymmetric slots [10, 11, 13] create two orthogonal electric field

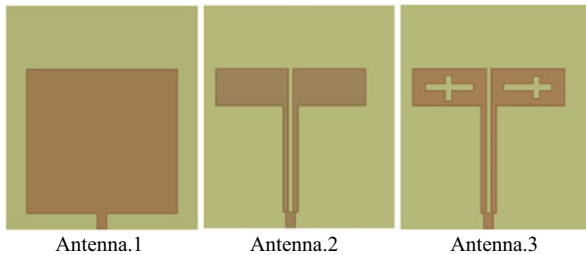


Fig. 1 Improvement of implemented antenna

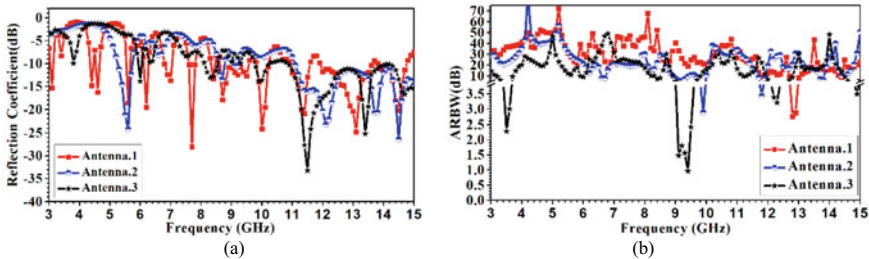


Fig. 2 Evaluation of a Reflection coefficient and b Axial ratio bandwidth for Antenna. 1–3

with equal amplitude at these two-resonating frequencies. But this Antenna.3 gives reflection coefficient is not so good in lower frequency region but moderate in higher frequency region. So, to identify the existing modes within the same radiator it is need to study TCM analysis of this radiator.

**TCM Analysis and Design of Proposed Antenna**

The TMA analysis is done by using the radiator without feeding structure [12, 14]. Here radiator is considered to be zero thickness with PEC and the ground plane, substrate is considered to be infinite and results are analysed in Figs. 3. Figure 3(a) described the plot of eigenvalues versus frequency plot of the fourteen fundamental characteristic modes. The eigenvalues ( $\lambda_n = 0$ ) for modes 2, 3, 5, 6, 7, 8, 9, 11, 12, 14, 15, 17 18, 22 are dominant modes, whereas no mode are inductive mode as it has very high eigenvalues ( $\lambda_n > 0$ ) and 1, 4, 10, 13, 16, 19, 20 and 21 modes are capacitive mode as it has low high eigenvalues ( $\lambda_n < 0$ ).

From Fig. 1(b) the plot of characteristics angle versus frequency plot of the fourteen fundamental characteristic modes. Here mode 2, 3, 5, 6, 7, 8, 9, 11, 12, 14, 15, 17 18, 22 are crosses  $180^\circ$  axis line at their resonant frequencies which are dominant modes. Whereas 1, 4, 10, 13, 16, 19, 20 and 21 modes are non-resonant modes as they doesn't cross  $180^\circ$  axis line.

Similarly Fig. 1(c) described large model significance value around 1 are dominant at their resonant frequencies for mode 2, 3, 5, 6, 7, 8, 9, 11, 12, 14, 15, 17 18, 22 and model significance ( $<0.2$ ) for 1, 4, 10, 13, 16, 19, 20 and 21 modes which are non-resonant modes.

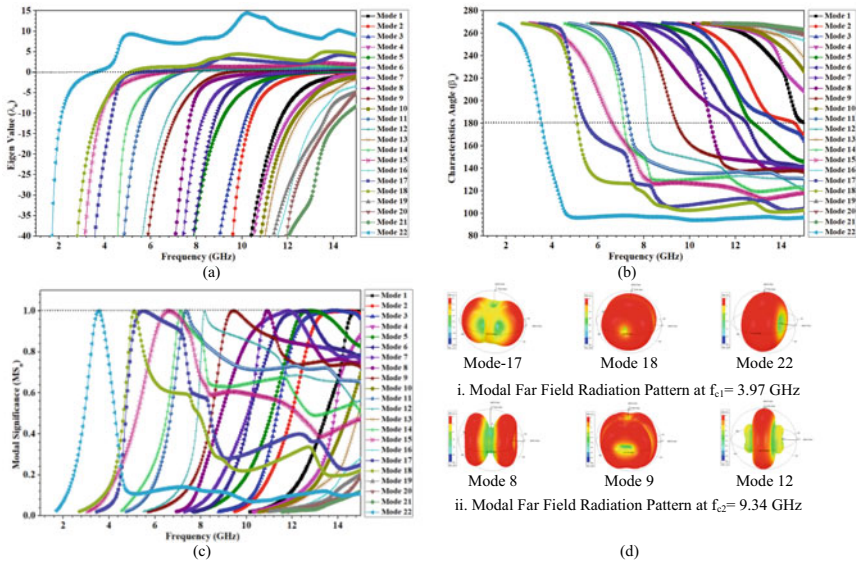


**Fig. 3** TCMs analysis for different modes **a** Eigen values, **b** Characteristics angle, **c** Modal significance and **d** Radiation pattern

From Fig. 3 after TCM analysis it has been revealed that there are 14 existing dominant modes within the radiator from 3–15 GHz resonating frequency region. The dominant modes of the radiator are resonating at 3.54 GHz (Modes 22), 5.09 GHz (Modes 18), 5.48 GHz (Modes 17), 6.63 GHz (Modes 15), 7.13 GHz (Modes 14), 7.36 GHz (Modes 11), 8.17 GHz (Modes 12), 9.44 GHz (Modes 9), 10.92 GHz (Modes 8), 11.85 GHz (Modes 7), 12.48 GHz (Modes 6), 12.78 GHz (Modes 5), 13.84 GHz (Modes 3), 14.58 GHz (Modes 2). So, from this TCM analysis it can be conclude that if one researcher design the feed and ground plane properly there may be the possibility to get good IBW within 3–15 GHz band region. After parametric analysis it is identified that asymmetric microstrip line feed and a defective ground plane [9] can be able to excite above dominant modes.

Two degenerated modes generate a CP mode when the phase among them is  $90^\circ$  and amplitude is equal.

Here Fig. 3d(i)–(ii) shows radiation pattern for modal far field of the radiator for different modes at two CP resonating Frequencies. Figure 4d(i) depicts that mode 18 and 22 radiate in  $+z$  direction at  $f_{c1} = 3.97$  GHz ad they are fundamental modes along y and x direction correspondingly. As the phase difference between them is  $90^\circ$  so these two orthogonal modes are able to generate a CP at  $f_{c1} = 3.97$  GHz resonating frequency. Figure 3d(ii) depicts that mode 9 and 12 radiate in  $+z$  direction at  $f_{c1} = 9.34$  GHz and they are fundamental modes along y and x direction correspondingly. As the phase difference between them is  $90^\circ$  so these two orthogonal modes are able to generate another CP at  $f_{c1} = 3.97$  GHz resonating frequency. The other Modes lead to cancelation of electric field in the far field zone at  $+z$  direction so they are undesired to generate CP mode.

The designed antenna simulated structures is shown in Fig. 3(a) and (b) and it helps to achieve quad impedance bands which are resonating at the centre frequencies of 3.9 GHz, 7.52 GHz, 9.56 GHz and  $>12.92$  GHz respectively and it's also give dual CP bands, resonating at 3.97 and 9.34 GHz, results shown in Fig. 4(a) and (b). Since it satisfied our purpose, it definite to select finalized this design and analysed its performance. The size of the microstrip antenna is  $70 \times 60$  mm<sup>2</sup>. Commonly available, low cost workable FR4-epoxy substrate thickness of 1.6 mm, having  $\epsilon_r =$

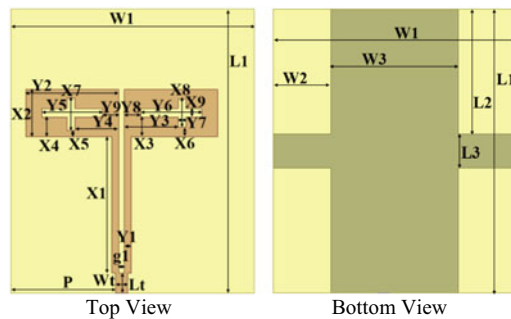


Fig. 4 Dimension of proposed antenna

**Table 1** Proposed antenna optimal dimension

Parameter	Value (mm)	Parameter	Value (mm)	Parameter	Value (mm)
L1	70	L2	30.9	L3	8.2
W1	60	W2	14.3	W3	31.4
Lt	5	Wt	3	g1	1.4
X1	33.5	X2	11.7	X3	4.8
X4	4.8	X5	1.7	X6	2.0
X7	7.8	X8	7.0	X9	2.1
Y1	1.7	Y2	23	Y3	13.2
Y4	10.8	Y5 = Y6	15	Y7	2.0
Y8 = Y9	4	P	25.8	h	1.6

4.4 and loss tangent  $\tan\delta = 0.02$  is utilized to simulated the implemented antenna. Comprehensive optimal dimensions have been recorded in Table 1.

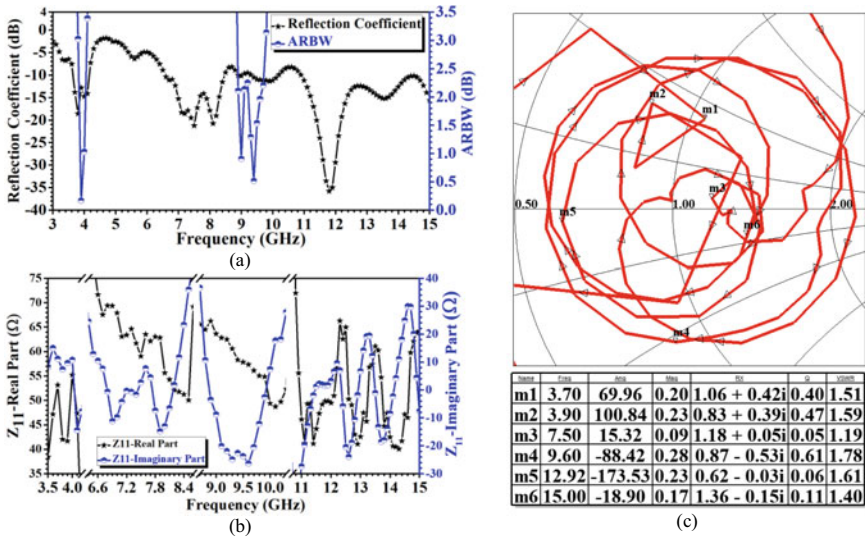
### 3 Simulation Justifications and Discussions

To design the antenna, use simulation software, Ansys Electronics Desktop 2020 R1. The designed antenna enclosed the quad simulated IBW ranged from 3.631–4.167 GHz (535.6 MHz,  $f_{rc1} = 3.9$  GHz, 13.73%), 6.542–8.494 GHz (1951.8 MHz,  $f_{rc2} = 7.52$  GHz, 25.96%), 8.859–10.253 GHz (1134.3 MHz,  $f_{rc3} = 9.56$  GHz, 14.59%) and 10.8494- beyond 15 GHz (4150.6 MHz,  $f_{rc4} = 12.92$  GHz, 32.19%) depicts in Fig. 5(a).

Figure 5(b) also depicts the simulated ARBW of the implemented antenna. The simulateddual ARBW span over 3.865–4.069 GHz (203.7 MHz,  $f_{cp1} = 3.97$  GHz, 5.14%) within 1<sup>st</sup> IB and 8.888–9.785 GHz (897.3 MHz,  $f_{cp2} = 9.34$  GHz, 9.6%) within 3<sup>rd</sup> IB.

Figure 5(b) simulated input impedance is depicting at 50  $\Omega$  microstrip feed line for the real (Resistance) and imaginary (Reactance) parts. Within the IBs impedance match is good because the real part (resistance) of the impedance closer to 50  $\Omega$  and the imaginary part (reactance) is closer to 0  $\Omega$ .

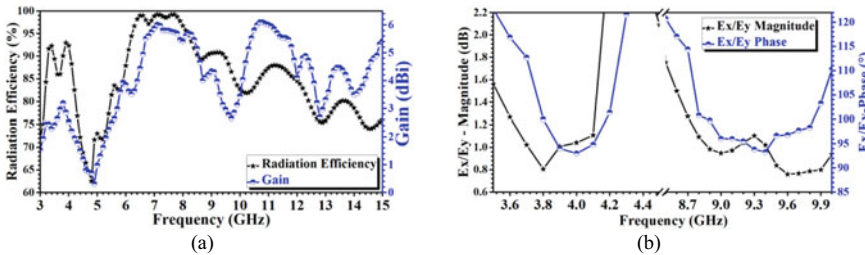
From Fig. 5(c) using smith chart one can see that on resonance frequency 3.7, 3.9, 7.5, 9.6, 12.92, and 15.0 GHz the normalized impedance ( $Z_{11}$ ) values are close to 1 whereas the complex reflection coefficient magnitude ( $\Gamma$ ) values are also very small. So above values depict that best matching can occur on resonance frequencies because real part of  $Z_{11}$  approaches to 50 $\Omega$  and imaginary part tends to 0 $\Omega$ . Also, VSWR value on those frequencies is also <2. The Q-value on those lower resonating frequencies in addition to higher resonating frequencies is also very small. That signify widest IBW can occur due to small Q-factor. At centre resonating frequencies also depicts that impedance matching can occur on those frequencies as VSWR value



**Fig. 5** (a) Simulated reflection coefficient and ARBW curves comparisons, (b) Simulated impedance (Real and Imaginary) vs. Frequency curves, (c) Results of the effect of complex reflection coefficient ( $\Gamma$ ), normalized input impedance ( $Z_{11}$ ), Q-factor and VSWR using Smith Chart for the Implemented Antenna

<2. From this Smith chart it's also clear that the graph rotates four times nearly equal to kick point (SWR = 1) which prove quad impedance bands are generate by using the same structure.

Figure 6(a) depicts the radiation efficiency (simulated) for the designed antenna respecting frequencies. The ranges of radiation efficiencies in between 74–99% for the quad IBs. The maximum efficiency is 99.17% at 7.1 GHz. Figure 6(a) also depicts the at peak gains respecting frequency. The gain is within 2.20–6.01 dBi for quad the impedance bands and the peak gain is maximum 6.01 dBi at 7.1 GHz.



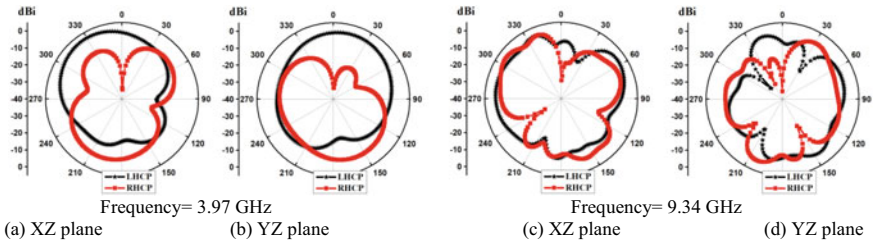
**Fig. 6** Implemented Antenna **a** Gain and radiation efficiency, **b**  $E_x/E_y$  magnitude and phase plot vs. Frequency



Figure 6(b) depicts the  $E_x/E_y$  magnitude is closely equal to 1 or 0 dB within the dual CP bands and phase difference among them is also nearly  $90^\circ$ . This demonstrates that the dual bands gratify CP conditions [13].

Well defined, LHCP and RHCP are detected in Fig 7(a), (c) and (b), (d) which are illustrating the radiation patterns at  $\varphi = 0^\circ$  (XZ plane) and  $\varphi = 90^\circ$  (YZ plane) at  $f_{cp1} = 3.97$  GHz and  $f_{cp2} = 9.34$  GHz. At broadside direction on two CP resonating frequencies the radiations observed are LHCP whereas the polarization (co and cross) difference are 32.47 dBi, and 22.57 dBi, correspondingly. Because of the asymmetric inset feeding radiator, the distribution of current is productive, due to that reason radiation is somewhat slanting from its broadside direction.

To understanding the generation of the dual CP modes at 3.97 and 9.34 GHz, a qualitative study is depicted in Fig. 8. The normalized currents distribution from the below figures it is observed that for four separate time moments ( $t = 0, t = T/4, t =$



**Fig. 7** Radiation patterns for (LHCP and RHCP) in the **a, c** XZ ( $\varphi = 0^\circ$ ) and **b, d** YZ ( $\varphi = 90^\circ$ ) planes

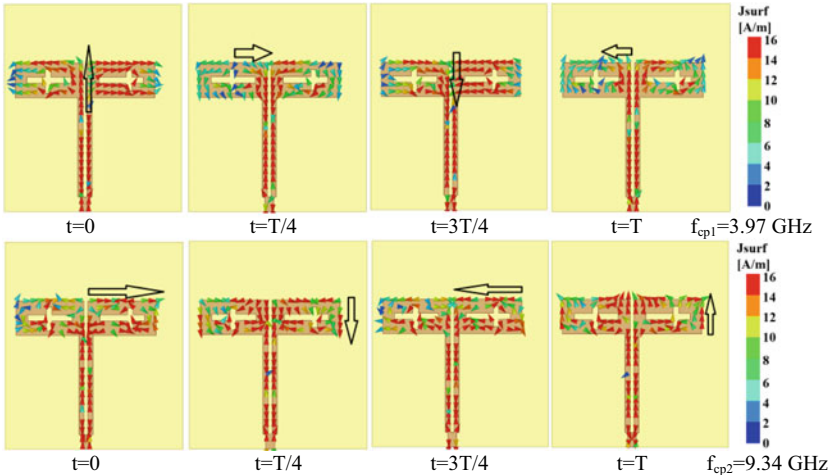


**Fig. 8** Simulated current distribution at  $f_{cp1} = 3.97$  GHz and at  $f_{cp2} = 9.34$  GHz



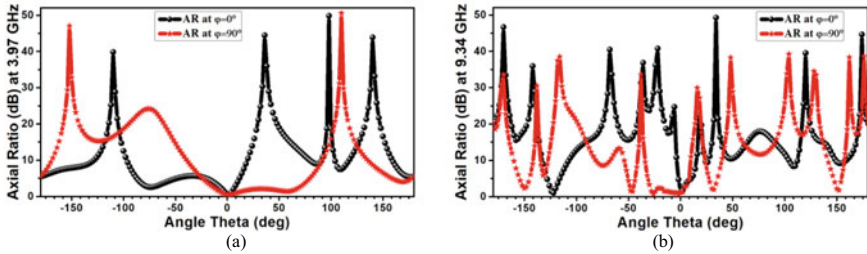


**Fig. 9** Axial ratio beam width vs.  $\theta^\circ$  at XZ plane ( $\varphi = 0^\circ$ ) and YZ plane ( $\varphi = 90^\circ$ ) **c**  $f_{cp1} = 3.97$  GHz, **b**  $f_{cp2} = 9.34$  GHz for the proposed antenna

3 T/4,  $t = T$  where for one cycle T is the total time period), dual CP modes could be accomplished at  $f_{cp1} = 3.97$  GHz,  $f_{cp2} = 9.34$  GHz which are LHCP.

The simulated axial ratio beam width  $f_{cp1} = 3.97$  GHz and  $f_{cp2} = 9.34$  GHz are plotted vs.  $\theta^\circ$  in Fig. 9(a) and (b). As obtained the results through simulation, at  $f_{cp1}$  the implemented antenna has a 3 dB AR beam width over vertical  $\theta$  angle of about  $17^\circ$  at XZ ( $\varphi = 0^\circ$ ) plane and  $89^\circ$  at YZ ( $\varphi = 90^\circ$ ) plane. So, at broadside direction the difference between co- and cross plane simulated 3 dB AR beam width is  $72^\circ$  at  $f_{cp1} = 3.97$  GHz. Similarly, at  $f_{cp2}$  the implemented antenna has a 3 dB AR beam width over vertical  $\theta$  angle of about  $5^\circ$  at XZ ( $\varphi = 0^\circ$ ) plane and  $35^\circ$  at YZ ( $\varphi = 90^\circ$ ) plane. So, at broadside direction the difference between co- and cross plane simulated 3 dB AR beam width is  $30^\circ$  at  $f_{cp2} = 9.34$  GHz.

## 4 Conclusion

In this paper TCM analysis helps to create a great extent simpler method to design a quad IB with polarization diversified monopole antenna assessment compare to former design techniques. The implemented antenna showing LHCP in 1<sup>st</sup> IB, LP in 2<sup>nd</sup> IB, LHCP in 3<sup>rd</sup> IB and LP in 4<sup>th</sup> IB are comprehended by employing changes in ground plane and asymmetric feeding network of two L-shaped planar monopole antenna with two asymmetric cross shaped slots. The proposed antenna (size  $70 \times 70$  mm<sup>2</sup> i.e.  $1.378 \times 1.181 \lambda_g^2$ ,  $\lambda_g =$  guided wavelength at 3.6 GHz) gives quad IBW, are 13.97, 25.96, 14.59 and 32.19% resonating at 3.9, 7.52, 9.56, and 12.92 GHz respectively. The dual CP bands of this antenna (5.14% at  $f_{cp1} = 3.97$  GHz and 9.6% at  $f_{cp2} = 9.34$  GHz) can support S- and X band specially FSS and SAR applications in a single device.

## References

1. Toh BY, Cahill R, Fusco VF (2003) Understanding and measuring circular polarization. *IEEE Trans Educ* 46(3):313–318. <https://doi.org/10.1109/TE.2003.813519>
2. Yu D, Gong SX, Xu Y, Wan YT (2015) Dual-band dual-polarized circular microstrip patch antenna with the curved slots on the ground. *Progr Electromagn Res* 51:27–31. <https://doi.org/10.2528/PIERL14112004>
3. Langston WL, Jackson DR (2004) Impedance, axial-ratio, and receive-power bandwidths of microstrip antennas. *IEEE Trans Antennas Propag* 52(10):2769–2774
4. Bao XL, Ammann MJ (2011) Wideband dual-frequency dual-polarized dipole-like antenna. *IEEE Antennas Wirel Propag Lett* 10:831–834. <https://doi.org/10.1109/LAWP.2011.2164609>
5. Ding K, Gao C, Wu Y, Qu D, Zhang B, Wang Y (2017) Dual-band and dual-polarized antenna with endfire radiation. *IET Microwaves Antennas Propag* 11(13):1823–1828. <https://doi.org/10.1049/iet-map.2017.0124>
6. Bag B, Biswas P, Biswas S, Sarkar PP (2019) Wide-bandwidth multifrequency circularly polarized monopole antenna for wireless communication applications. *Int J RF Microwave Comput Aided Eng* 29(3):e21631. <https://doi.org/10.1002/mmce.21631>
7. Madaka KCR, Muthusamy P Mode investigation of parasitic annular ring loaded dual band coplanar waveguide antenna with polarization diversity characteristics. *Int J RF Microwave Comput Aid Eng* e22119. <https://doi.org/10.1002/mmce.22119>
8. Dhara R, Jana SK, Mitra M (2020) Tri-band circularly polarized monopole antenna for wireless communication application. *Radioelectron Commun Syst* 63(4):213–222. <https://doi.org/10.3103/S0735272720040044>
9. Dhara R (2021) A compact dual band dual polarized monopole antenna with enhanced bandwidth for C, X, and Ku band applications. *Progr Electromagn Res Lett* 96:65–72. <https://doi.org/10.2528/PIERL20121903>
10. Singh AK, Patil S, Kanaujia BK, Pandey VK (2020) A novel printed circularly polarized asymmetric wide slot antenna for digital cellular system. *Microw Opt Technol Lett* 62(3):1438–1447. <https://doi.org/10.1002/mop.32177>
11. Ellis MS, Effah FB, Ahmed AR, Kponyo JJ, Nourinia J, Ghobadi C, Mohammadi B (2020) Asymmetric circularly polarized open-slot antenna. *Int J RF Microwave Comput Aided Eng* 30(5):e22141. <https://doi.org/10.1002/mmce.22141>
12. Dhara R, Yadav S, Sharma MM, Jana SK, Govil MC (2021) A circularly polarized quad-band annular ring antenna with asymmetric ground plane using theory of characteristic modes. *Progr Electromagn Res* 100:51–68. <https://doi.org/10.2528/PIERM20102006>
13. Dhara R, Mitra M (2020) A triple-band circularly polarized annular ring antenna with asymmetric ground plane for wireless applications. *Eng Rep* 2(4):e12150. <https://doi.org/10.1002/eng2.12150>
14. Dhara R (2021) Design of a miniaturized CPW fed Z-shaped monopole antenna using theory of characteristics modes for bandwidth enhancement. *Sādhanā* 46(2):1–14. <https://doi.org/10.1007/s12046-021-01610-7>